

Distortion-free gain and noise correlation in sodium vapor with four-wave mixing and coherent population trapping

T. T. Grove and M. S. Shahriar

Research Laboratory of Electronics, Massachusetts Institute of Technology, Cambridge, Massachusetts 02138

P. R. Hemmer

Rome Laboratory, Hanscom Air Force Base, Massachusetts 01731

Prem Kumar

Department of Electrical Engineering and Computer Science, Northwestern University, Evanston, Illinois 60208

V. S. Sudarshanam, and M. Cronin-Golomb

Electro-Optics Technology Center, Tufts University, 6 Colby Street, Medford, Massachusetts 02155

Received January 10, 1997

We observed optical gain as great as 30 with nearly distortion-free beam propagation in optically dense sodium vapor, using four-wave mixing. Moreover, 15-dB classical noise correlations were seen in the amplified probe and conjugate beams. To achieve this performance in such a strongly absorbing medium, one must suppress unwanted absorption and self-focusing effects. This is accomplished with coherent population trapping. © 1997 Optical Society of America

Phase conjugation by four-wave mixing (FWM) has numerous potential applications to image amplification, processing, and aberration correction.¹ In addition, FWM is a natural choice for the generation of spatially broadband squeezed light for sub-shot-noise imaging applications.^{2,3} In general, however, these applications require a FWM mechanism that can deliver high gain without propagation distortion or excessive scattered-light generation. For low-light-level imaging applications, the FWM should also be optimized for low-intensity cw signals.

Atomic vapors can provide the necessary gain for weak signals but tend to produce propagation distortion and scattered light.⁴ Recently it was shown that propagation distortion in optically dense atomic vapor can be eliminated by electromagnetically induced transparency,⁵ which in this context can be viewed as coherent population trapping⁶ (CPT) applied to optically dense samples. However, no amplification of the probe was observed. In Ref. 7 we demonstrated that high gain at low pump intensity can be obtained in optically dense sodium vapor, using FWM by CPT. Here we show that under optimum conditions, high gain and low spatial distortion can be achieved simultaneously. In addition, strong correlations in the intensity noises of the amplified probe and the conjugate are seen.

Figure 1(a) shows the sodium energy levels for the D_1 transition. The phase-conjugate FWM setup is shown in Fig. 1(b), in which F, B, P, and C denote the forward and backward pumps, the probe, and the conjugate, respectively. Pump beams F and B are produced by separate dye lasers but are adjusted to have nearly identical power (100 mW) and beam diameter (1.4 mm FWHM) and are both collimated to within 1 mrad. This corresponds to a pump inten-

sity of $\sim 4 \text{ W/cm}^2$, which is much lower than that required for achieving gain with other FWM mechanisms in sodium vapor.^{8,9} The approximate laser detunings shown in Fig. 1(a) apply only to zero-velocity atoms. The Doppler width of sodium is $\sim 1 \text{ GHz}$. The probe beam, P, is generated with an acousto-optic modulator driven near 1.77-GHz sodium hyperfine frequency. This probe beam has $\sim 1 \text{ mW}$ of optical power and a FWHM beam diameter of 0.9 mm. The angles between F and P (and B and C) are kept below 4 mrad

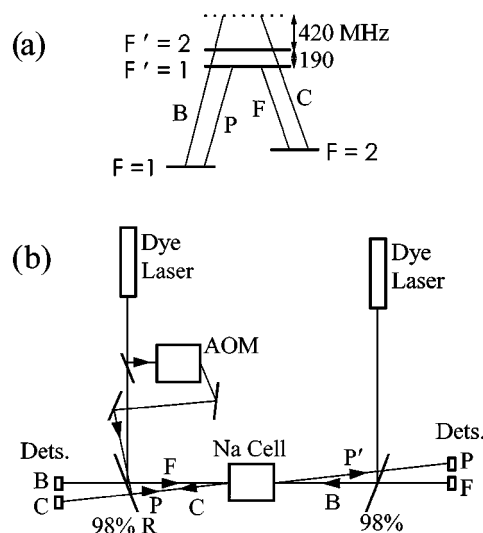


Fig. 1. (a) Sodium levels and approximate laser detunings for zero-velocity atoms. The ground state is $3^2S_{1/2}$, and the excited state is $3^2P_{1/2}$. (b) Schematic of the experimental setup. AOM, acousto-optic modulator; Dets., detectors.

to maintain good beam overlap over the active length of the sodium cell and to cancel Doppler shifts for the two-photon (Raman) transitions. The sodium cell is a heat pipe oven operated at $\sim 180^\circ\text{C}$ with an active length of ~ 5 cm. At this temperature, the (near-resonant) absorption of the probe beam is greater than 95%, when both pump beams are blocked.

Figure 2 shows the measured two-dimensional (left) and one-dimensional (right) spatial profiles of the transmitted probe beam ~ 1.2 m after passing through the cell. Transmitted probe-beam profiles are shown rather than conjugate profiles because they are a more sensitive measure of propagation distortion, owing to the fact that the phase conjugation automatically corrects for minor aberrations. Figure 2(a) shows the spatial profile for an unamplified probe when its frequency is tuned outside the Doppler-broadened sodium absorption line. The measured spot size is slightly larger than the 0.9-mm FWHM diameter in the cell center because of diffraction. Figure 2(b) shows the spatial profile of the transmitted probe when the optical power gain is 6. The smaller diameter in this case is attributed to slight self-focusing, which is noticeable only because of the large (1.2-m) cell-camera distance. The important point to note is the lack of visible aberrations or propagation distortions under these high-gain conditions. This result is to be contrasted with those of previous experiments using FWM in sodium vapor, in which strong signal distortion and self-focusing effects for gains of more than 2.5 were reported.⁹

Figure 2(c) shows the probe-beam profile when the optical power gain is 30. Here, propagation distortion effects are just becoming visible, as evidenced by asymmetries in the one- and two-dimensional spatial profiles. Such distortions become more severe for larger optical power gains (not shown); the largest power gain observed so far is >1000 . To obtain the high gain in Fig. 2(c), it was necessary for us to attenuate the input probe by a factor of 10 to overcome the gain limitation imposed by strong pump depletion. Finally, to verify that CPT is present, we measured the two-photon (Raman) linewidth by scanning the frequency difference between the F and the P lasers. The measured 4-MHz width is significantly narrower than the 10-MHz natural width of sodium and is taken as evidence of CPT.

In addition to spatial distortions, frequency and intensity noise can also affect the performance of an optical amplifier. Frequency-noise measurements for a probe-power gain of 10 are shown in Fig. 3. Initially, there are strong frequency correlations (2-kHz-wide beat) between pump F and unamplified probe P, since P is derived from F by use of an acousto-optic modulator. In contrast, the pump lasers F and B are uncorrelated (50-MHz-wide beat) since they are derived from separate unstabilized dye lasers. In spite of this lack of pump-frequency correlation, a narrow 2-kHz-wide beat note is still seen when F and amplified probe P' are beaten together and also when B and C are compared. Thus, the amplification process does not add noticeable frequency noise, even with separate unstabilized pump lasers.

Intensity-noise measurements for a probe-power gain of 20 are shown in Fig. 4. Figures 4(b) and 4(c) show the intensity-noise spectra of the conjugate (C) and amplified probe (P') beams, respectively. These are to be compared with the noise spectra of pumps B and F in Fig. 4(e) and 4(f), respectively, which were sampled before they passed through the cell and were adjusted to have the same power as C (and P'). As can be seen, the amplification process adds an average of 3 dB of intensity noise (at a noise frequency of 300 kHz). For reference, Fig. 4(a) shows the spectrum-analyzer noise floor. The intensity noise of the unamplified probe is below the noise floor.

In ideal FWM it is expected that quantum-noise correlations between the amplified probe and the conjugate beams (squeezing) will occur.¹⁰ For the system in Fig. 1(a), we have shown theoretically¹¹ that the conjugate and the amplified probe are twin beams, with noise correlations as low as 10 dB below the shot-noise

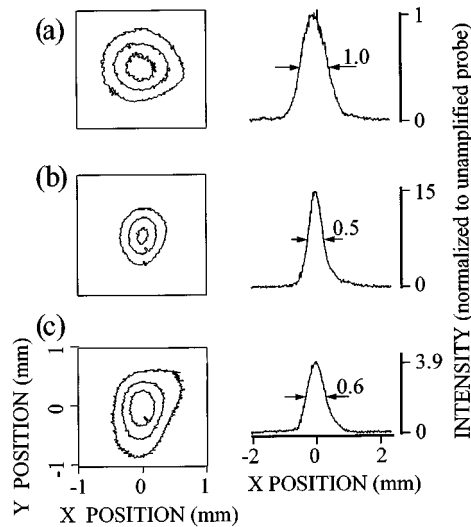


Fig. 2. Two-dimensional contour plots (left) and one-dimensional line traces (right) showing spatial profiles of transmitted probe beams. Contour lines correspond to 29%, 57%, and 86% of maximum intensity. (a) Unamplified probe, (b) probe-power gain of 6, (c) probe-power gain of 30.

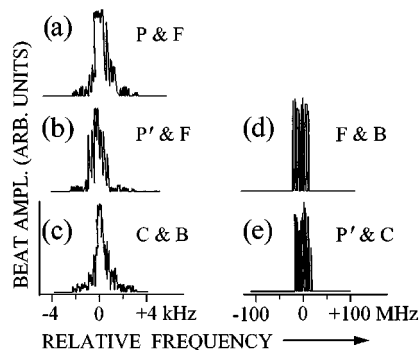


Fig. 3. Beat notes between labeled beams (P' denotes the amplified probe). The approximate spectrum analyzer settings are (a)–(c) center frequency 1.77 GHz, bandwidth 1 kHz, (d) and (e) center frequency 1.45 GHz, bandwidth 1 MHz.

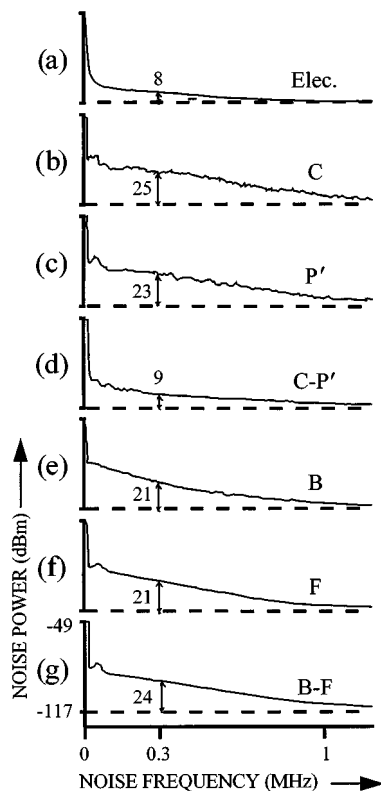


Fig. 4. Photocurrent noise versus frequency for labeled beams. Probe and conjugate beams are sampled after transmission through a 98% reflectivity beam splitter. The transimpedance amplifier gain is 10^4 V/A, the spectrum-analyzer reference level is -49 dBm, and the bandwidth is 10 kHz. (a) Spectrum-analyzer noise floor; (b) conjugate noise; (c) amplified probe noise; (d) noise in subtracted photocurrents of the conjugate and the amplified probe; (e) and (f) backward and forward pump noise, respectively, when powers match that of the conjugate beam (sampled before it enters the sodium cell); (g) noise in subtracted photocurrents of the forward and the backward pumps.

limit. These noise correlations can be observed in the difference current of two photodiodes, one detecting the amplified probe and the other detecting the conjugate. So far, however, we have observed only classical noise correlations because of the large amount of classical (technical) noise generated by the dye lasers. This is shown in Fig. 4(d), which shows the noise on the dif-

ference photocurrent $C-P'$. By comparing Figs. 4(b)–4(d), we estimate noise correlations of 15 dB at a noise frequency of 300 kHz. In comparison, Fig. 4(g) shows the noise on the difference photocurrent for pumps B–F. In this case the noise increases, as expected.

In an attempt to detect quantum-noise correlations, we directed the full power of the probe and the conjugate beams into the photodetectors and looked at higher noise frequencies, in analogy to previous noise-correlation measurements in atomic vapor.¹² Unfortunately, the intensity-noise correlations decreased rapidly as the noise frequency increased. For example, at a noise frequency of 2 MHz, which is close to the 4-MHz Raman linewidth, the correlation is only ~ 3 dB, compared with 15 dB at 300 kHz. However, our dye laser classical noise extends well beyond 2 MHz, and hence we were unable to look for quantum-noise correlations.

In conclusion, we have demonstrated a high-gain FWM technique that yields distortion-free propagation in optically dense atomic vapor at low pump intensity. Furthermore, there is a high degree of intensity-noise correlation between the amplified probe and the conjugate beams.

References

1. R. Fisher, ed., *Optical Phase Conjugation* (Academic, New York, 1983).
2. P. Kumar and M. I. Kolobov, *Opt. Commun.* **104**, 374 (1994).
3. M. I. Kolobov and P. Kumar, *Opt. Lett.* **18**, 849 (1993).
4. S. T. Ho, P. Kumar, and J. H. Shapiro, *J. Opt. Soc. Am. B* **8**, 37 (1991).
5. M. Jain, A. J. Merriam, A. Kasapi, G. Y. Yin, and S. E. Harris, *Phys. Rev. Lett.* **75**, 4385 (1995).
6. E. Arimondo, in *Progress in Optics XXXV*, E. Wolf, ed. (Elsevier, New York, 1996), pp. 258–354.
7. P. R. Hemmer, D. P. Katz, J. Donoghue, M. Cronin-Golomb, M. S. Shahriar, and P. Kumar, *Opt. Lett.* **20**, 982 (1995).
8. M. Vallet, M. Pinard, and G. Grynberg, *Opt. Commun.* **81**, 403 (1991).
9. J. R. R. Leite, P. Simoneau, D. Bloch, S. Le Boiteux, and M. Ducloy, *Europhys. Lett.* **2**, 747 (1986).
10. H. P. Yuen and J. H. Shapiro, *Opt. Lett.* **4**, 334 (1979).
11. M. S. Shahriar and P. R. Hemmer, in *Coherence and Quantum Optics VII*, J. H. Eberly, L. Mandel, and E. Wolf, eds. (Plenum, New York, 1996), pp. 479–480.
12. M. Kauranen and R. W. Boyd, *Phys. Rev. A* **47**, 4297 (1993).